

# Arginine-Containing Ligands Enhance H<sub>2</sub> Oxidation Catalyst Performance\*\*

Arnab Dutta, John A. S. Roberts,\* and Wendy J. Shaw\*

**Abstract:** Hydrogenase enzymes use Ni and Fe to oxidize H<sub>2</sub> at high turnover frequencies (TOF) (up to 10000 s<sup>-1</sup>) and low overpotentials (< 100 mV). In comparison, the fastest reported synthetic electrocatalyst, [Ni<sup>II</sup>(P<sup>Cy</sup><sub>2</sub>N<sup>tBu</sup><sub>2</sub>)<sub>2</sub>]<sup>2+</sup>, oxidizes H<sub>2</sub> at 60 s<sup>-1</sup> in MeCN under 1 atm H<sub>2</sub> with an unoptimized overpotential of ca. 500 mV using triethylamine as a base.<sup>[1]</sup> Here we show that a structured outer coordination sphere in a Ni electrocatalyst enhances H<sub>2</sub> oxidation activity: [Ni<sup>II</sup>(P<sup>Cy</sup><sub>2</sub>N<sup>Arg</sup><sub>2</sub>)<sub>2</sub>]<sup>8+</sup> (Arg = arginine) has a TOF of 210 s<sup>-1</sup> in water with high energy efficiency (180 mV overpotential) under 1 atm H<sub>2</sub>, and 144000 s<sup>-1</sup> (460 mV overpotential) under 133 atm H<sub>2</sub>. The complex is active from pH 0–14 and is faster at low pH, the most relevant condition for fuel cells. The arginine substituents increase TOF and may engage in an intramolecular guanidinium interaction that assists in H<sub>2</sub> activation, while the COOH groups facilitate rapid proton movement. These results emphasize the critical role of features beyond the active site in achieving fast, efficient catalysis.

Enzymes perform challenging bond formation and cleavage, electron transfer, atom transfer and radical reactions with impressive ease.<sup>[2]</sup> The protein scaffold or outer coordination sphere of the enzyme controls dynamic switching processes, local pH, polarity, electrochemical potential, and the transport of reactants and products over long distances, making enzymes more active and selective than synthetic analogs.<sup>[2]</sup> The outstanding performance of these naturally occurring catalysts has inspired a biomimetic approach to the development of synthetic catalyst systems.<sup>[3]</sup>

Hydrogenases are a class of metalloenzymes that use abundant metals such as Ni and Fe to interconvert protons and electrons with H<sub>2</sub>, reactions that hold promise for the

storage and recovery of intermittent sources of electricity such as solar and wind.<sup>[4]</sup> The protein scaffold transports H<sub>2</sub>, protons, and electrons, and controls the environment around the active site,<sup>[4]</sup> resulting in rapid turnover (up to ca. 10000 s<sup>-1</sup> for H<sub>2</sub> oxidation)<sup>[6a]</sup> with minimal excess driving force or overpotential,<sup>[5]</sup> meaning that they are also energy-efficient.<sup>[4,6]</sup>

Recently, we reported the first water-soluble H<sub>2</sub> oxidation catalyst, [Ni<sup>II</sup>(P<sup>Cy</sup><sub>2</sub>N<sup>Gly</sup><sub>2</sub>)<sub>2</sub>]<sup>4+</sup> (Cy = cyclohexyl, Gly = glycine), with a simple two-component proton channel involving both the amines and carboxylic acids of glycine (Figure 1).<sup>[7]</sup> It is

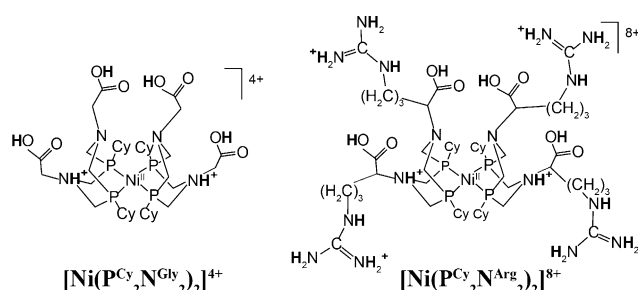


**Figure 1.** Complexes [Ni<sup>II</sup>(P<sup>Cy</sup><sub>2</sub>N<sup>Gly</sup><sub>2</sub>)<sub>2</sub>]<sup>4+</sup> and [Ni<sup>II</sup>(P<sup>Cy</sup><sub>2</sub>N<sup>Arg</sup><sub>2</sub>)<sub>2</sub>]<sup>8+</sup> at acidic pH with exchangeable protons as a function of pH shown in bold.

catalytic from pH 0.1 to 8.5, with maximum activity at pH 0.7 (1 atm H<sub>2</sub>) of 33 s<sup>-1</sup> and an overpotential at E<sub>cat/2</sub> (the potential at one half of the maximum catalytic current) of 150 mV,<sup>[7]</sup> placing it among the fastest and most energy-efficient H<sub>2</sub> oxidation catalysts reported.<sup>[1,8]</sup> Electrochemical and IR spectroscopic measurements demonstrate rapid proton exchange between the pendant amines and the glycine COOH groups,<sup>[7]</sup> suggesting that facilitating proton movement may also provide a way to decrease the overpotential required for catalysis.

Here we report [Ni<sup>II</sup>(P<sup>Cy</sup><sub>2</sub>N<sup>Arg</sup><sub>2</sub>)<sub>2</sub>]<sup>8+</sup> (Figure 1),<sup>[9]</sup> a complex containing the amino acid arginine instead of glycine. [Ni<sup>II</sup>(P<sup>Cy</sup><sub>2</sub>N<sup>Arg</sup><sub>2</sub>)<sub>2</sub>]<sup>8+</sup> is water soluble and functions as an H<sub>2</sub> oxidation electrocatalyst from pH 0–14. It operates at higher turnover frequencies than [Ni<sup>II</sup>(P<sup>Cy</sup><sub>2</sub>N<sup>Gly</sup><sub>2</sub>)<sub>2</sub>]<sup>4+</sup>, and both turnover frequency and overpotential are correlated with the protonation state of the complex, with the protonated forms of the carboxylic acid and guanidinium groups resulting in the best catalytic performance. While the guanidinium groups at the periphery of the molecule can act to shuttle protons via a Grotthuss mechanism<sup>[10]</sup> as suggested in some proteins,<sup>[11]</sup> our data shows that these groups may be forming a strong Arg–Arg interaction that contributes to enhanced catalytic activity.<sup>[12]</sup>

[\*] Dr. A. Dutta, Dr. J. A. S. Roberts, Dr. W. J. Shaw  
Pacific Northwest National Laboratory  
902 Battelle Blvd., Richland, WA 99352 (USA)  
E-mail: John.Roberts@pnnl.gov  
Wendy.Shaw@pnnl.gov

[\*\*] We would like to thank Dr. Daniel DuBois for useful discussions. This work was funded by the Office of Science Early Career Research Program through the US DOE, BES (A.D., W.J.S.), and the Center for Molecular Electrocatalysis, an Energy Frontier Research Center funded by the US DOE, BES (J.A.S.R.). Part of the research was conducted at the W.R. Wiley Environmental Molecular Sciences Laboratory, a national scientific user facility sponsored by US DOE's Office of Biological and Environmental Research program located at Pacific Northwest National Laboratory (PNNL). PNNL is operated by Battelle for the US DOE. We thank Dr. Charles Weiss and Dr. Jonathan Darmon for the preparation of the table-of-contents graphic.

Supporting information for this article is available on the WWW under <http://dx.doi.org/10.1002/anie.201402304>.

We have incorporated arginine into the eight-membered heterocyclic  $P_2N_2$  (1,5-diaza-3,7-diphosphacyclooctane) ligand following previously reported syntheses<sup>[7–8]</sup> to obtain  $P^{Cy}_2N^{Arg}_2$ , which binds  $Ni^{II}$  in methanol to produce the  $[Ni^{II}(P^{Cy}_2N^{Arg}_2)_2]^{8+}$  complex (Figure 1). Characterization by  $^1H$  NMR,  $^{31}P$  NMR, and mass spectrometry is consistent with this complex and is similar to analogous complexes.<sup>[1,7–8]</sup> The cyclic voltammetry in water under  $N_2$  (Figure 2 A) shows two overlapping one-electron waves corresponding to the  $Ni^{II/I}$  and  $Ni^{I/0}$  redox couples, as observed with  $[Ni(P^{Cy}_2N^{Gly}_2)_2]^{4+}$ .<sup>[7]</sup>

Adding  $H_2$  (1 atm) to  $[Ni^{II}(P^{Cy}_2N^{Arg}_2)_2]^{8+}$  in unbuffered aqueous solution (pH 4.0) produces a current enhancement corresponding to electrocatalytic oxidation of  $H_2$ , with water acting as the base (similar observations were made for the buffered solution; Figure 2). The maximum current ( $i_{cat}$ ,

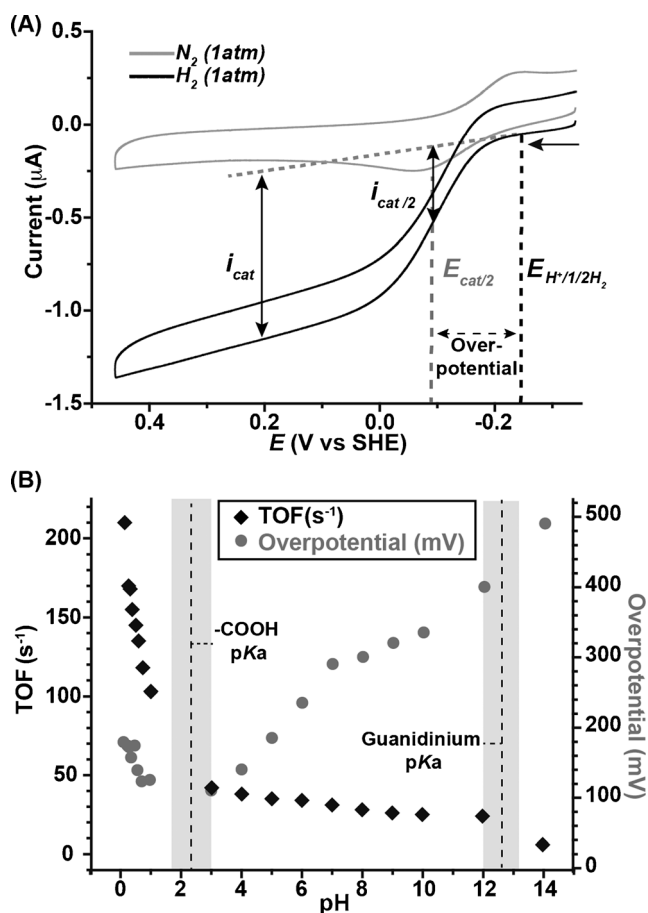


**Figure 2.** A) Cyclic voltammetry of  $50\ \mu M$   $[Ni^{II}(P^{Cy}_2N^{Arg}_2)_2]^{8+}$  under  $N_2$  (gray) and 1 atm  $H_2$  (black) at pH 4 in aqueous  $0.1\ M\ Na_2SO_4/0.1\ M$  MES/HEPES buffer demonstrates catalytic activity under  $H_2$ . The angled dashed line represents the background current; the vertical black arrows show  $i_{cat}$  (catalytic current) and  $i_{cat/2} = 1/2 i_{cat}$ ;  $E_{cat/2}$  is the corresponding half-peak potential (gray dotted line).  $E_{H^+/1/2H_2}$  is the equilibrium potential for the reaction being mediated (black dotted line). The difference between these is the overpotential at  $E_{cat/2}$ . The solid horizontal black arrow indicates the initial scan direction. Data were taken at  $0.2\ V s^{-1}$  using a glassy carbon electrode. B) Dependence of turnover frequency and overpotential on pH at 1 atm  $H_2$ . The black vertical dotted lines indicate the experimentally determined  $pK_a$  values of the COOH and guanidinium groups, with the surrounding gray regions indicating the error associated with those values.

defined in Figure 2) is independent of the potential sweep rate ( $v = 0.1$ – $1.0\ V s^{-1}$ , Figure S1 in the Supporting Information), consistent with catalysis at steady state, with the rate controlled by chemical steps rather than substrate diffusion.<sup>[13]</sup> The catalytic current increases linearly with catalyst concentration (Figure S1), and catalysis is homogeneous based on the rinse test (Figure S2).<sup>[14]</sup> Therefore the TOF can be calculated from  $i_{cat}$  using Equation (1),<sup>[15]</sup>

$$TOF = \left( \frac{i_{cat}}{nFA[cat]\sqrt{D_{cat}}} \right)^2 \quad (1)$$

$D$  (diffusion coefficient of the catalyst;  $2.8 \times 10^{-6}\ cm^2 s^{-1}$ , see Supporting Information),  $A$  (electrode surface area;  $9.23 \times 10^{-3}\ cm^2$ ),<sup>[7]</sup>  $n$  (number of electrons; two), and  $F$  (Faraday's constant).

$[Ni^{II}(P^{Cy}_2N^{Arg}_2)_2]^{8+}$  oxidizes  $H_2$  to protons from pH 0 to pH 14 (Figure 2 B and S3). As shown in Figure 2 B, the TOF is lowest at pH > 12 ( $5\ s^{-1}$ ), increases five times on lowering the pH from 14 to 12, and increases gradually (1.4 times) upon lowering the pH from 12 to 3. The catalytic activity increases sharply under strongly acidic conditions (pH < 3), reaching a maximum TOF of  $210\ s^{-1}$  at pH  $\approx 0.1$ . The  $pK_a$  values of  $[Ni^{II}(P^{Cy}_2N^{Arg}_2)_2]^{8+}$ ,  $\approx 2.5$ , 7.0, and 12.5 (obtained by titration; Figure S4) correspond to deprotonation of the COOH groups, the pendant amines<sup>[16]</sup> and the guanidinium groups, respectively. The correlation of these  $pK_a$  values with the inflection points in the evolution of TOF with pH (Figure 2 B) indicates that the protonation state of the catalyst influences the catalytic pathway in specific ways. The overpotential for catalysis is also correlated strongly with protonation state. Overpotential is determined by taking the difference between the equilibrium potential [ $E_{H^+/1/2H_2}$ ; Eq. (S2)] and the catalytic potential ( $E_{cat/2}$ ; defined as the potential where the catalytic current is 50% of the maximum catalytic current  $i_{cat}$ ; Figure 2 A). Values ranged from 100–200 mV at low pH (the fastest turnover), and up to 500 mV at high pH.

$[Ni^{II}(P^{Cy}_2N^{Arg}_2)_2]^{8+}$  remains active under a variety of conditions known to quench either [NiFe]- or [FeFe]-hydrogenase enzymatic activity.<sup>[18]</sup>  $[Ni^{II}(P^{Cy}_2N^{Arg}_2)_2]^{8+}$  is stable under strongly acidic conditions (pH  $\approx 0$ ), showing only a 7% loss in catalytic activity after 24 h in the presence of the superacid bis(trifluoromethanesulfonyl)amine (HTFSI; Figure S5).<sup>[19]</sup>  $[Ni^{II}(P^{Cy}_2N^{Arg}_2)_2]^{8+}$  is sensitive to oxygen under extreme conditions, but still retains 20% reactivity after purging for 10 min with  $H_2$ :air (1:1; contains 10%  $O_2$ ) and requires 40 min purging to completely lose its reactivity (Figure S5).  $[Ni^{II}(P^{Cy}_2N^{Arg}_2)_2]^{8+}$  can oxidize  $H_2$  even in the presence of CO (Figure S5), as expected based on the reversibility of CO binding observed with other  $[Ni^{II}-(P^{Cy}_2N^{R'}_2)_2]^{2+}$  complexes in the presence of  $H_2$ .<sup>[1,20]</sup>

The value of TOF increases linearly with increasing  $H_2$  pressure up to 100 atm (Figure 3 B), beyond which TOF becomes independent of the  $H_2$  pressure at all pH values examined (0.4, 4.0, 9.0, and 14.0; Figure S6). Similar substrate saturation kinetics have been observed with analogous  $H_2$  production catalysts and are consistent with a first order dependence on  $H_2$  up to 100 atm and a zero order dependence beyond this.<sup>[21]</sup> Turnover is fastest at pH 0.4 (unbuffered

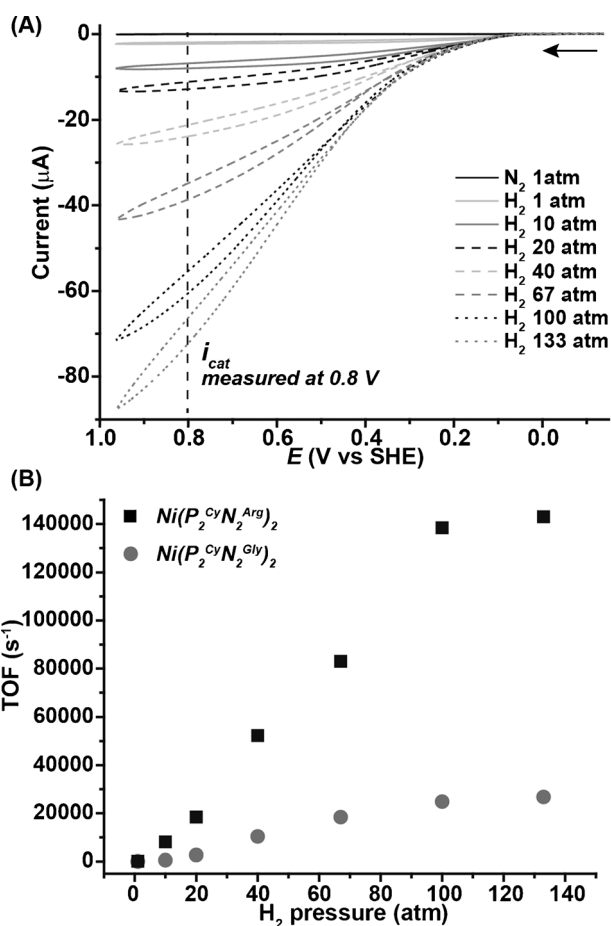


**Figure 3.** A)  $\text{H}_2$  oxidation catalysis by  $22 \mu\text{M}$   $[\text{Ni}^{\text{II}}(\text{P}^{\text{Cy}_2\text{N}^{\text{Arg}}_2})_2]^{8+}$  at pH 0.4 at increasing pressures of  $\text{H}_2$  (pH 0.4, 0.1 M  $\text{Na}_2\text{SO}_4$ ; the black arrow shows the initial scanning direction) and B) comparison of TOF for  $[\text{Ni}^{\text{II}}(\text{P}^{\text{Cy}_2\text{N}^{\text{Arg}}_2})_2]^{8+}$  and  $[\text{Ni}^{\text{II}}(\text{P}^{\text{Cy}_2\text{N}^{\text{Gly}}_2})_2]^{4+}$  (pH 0.7, 0.1 M  $\text{Na}_2\text{SO}_4$ ) at different pressures of  $\text{H}_2$ . Scan rate  $0.05 \text{ V s}^{-1}$ .  $i_{\text{cat}}$  was measured as indicated for all  $\text{H}_2$  pressures.

$\text{HClO}_4$ ) under 133 atm  $\text{H}_2$ , with  $\text{TOF} = 144\,000 \text{ s}^{-1}$  at 133 atm  $\text{H}_2$  ( $i_{\text{cat}}$  was measured at 0.8 V vs. SHE) (Figure 3), at an overpotential at  $E_{\text{cat}/2}$  of 460 mV. The waves become non-sigmoidal at higher pressures, possibly because electron transfer is rate-limiting over a wide potential range at higher TOF values, or because the  $\text{H}_2$  pressure influences the competition between catalytic pathways.<sup>[22]</sup> As observed for data collected at 1 atm  $\text{H}_2$ , the TOF is independent of catalyst concentration (0.08–22  $\mu\text{M}$ ; pH 0.4; up to 133 atm  $\text{H}_2$ ; Figure S1). With HTFSI rather than  $\text{HClO}_4$  as the acid, the catalyst demonstrated similar  $\text{H}_2$  oxidation activity with a maximum TOF of  $125\,000 \text{ s}^{-1}$  and an overpotential of 490 mV at 133 atm  $\text{H}_2$  (pH  $\approx 0$ ). Control experiments confirmed that  $\text{H}_2$  oxidation activity is due to the catalyst in solution, not deposited on the electrode surface (Figure S7) in agreement with results obtained at 1 atm  $\text{H}_2$ , and that catalysis is mediated neither by the glassy carbon electrode itself nor by  $\text{Ni}^{\text{II}}$  dissociated from the phosphine ligands (Figure S7).<sup>[14]</sup> The TOF at 133 atm,  $144\,000 \text{ s}^{-1}$ , may be the maximum achievable for this catalyst, however higher

pressures were not available with the current experimental setup to confirm this hypothesis.

Turnover is five to six times faster with the  $[\text{Ni}^{\text{II}}(\text{P}^{\text{Cy}_2\text{N}^{\text{Arg}}_2})_2]^{8+}$  complex (pH = 0.4) than with  $[\text{Ni}^{\text{II}}(\text{P}^{\text{Cy}_2\text{N}^{\text{Gly}}_2})_2]^{4+}$  (pH = 0.7) at all pressures examined (Figure 3B), indicating that the guanidinium groups play a unique role in enhancing TOF. The addition of free arginine to  $[\text{Ni}^{\text{II}}(\text{P}^{\text{Cy}_2\text{N}^{\text{Gly}}_2})_2]^{4+}$  did not result in rate enhancements, confirming that appended arginines are necessary. The sharp increase in TOF with decreasing pH observed near the  $\text{pK}_a$  of the guanidinium group (12.5; Figure 2B) suggests that the protonated form in particular is required for fast turnover.

Interactions between guanidinium groups (Arg–Arg pairing), employed as structural elements in many proteins,<sup>[12a,b,23]</sup> may also be relevant in  $[\text{Ni}^{\text{II}}(\text{P}^{\text{Cy}_2\text{N}^{\text{Arg}}_2})_2]^{8+}$ . We examined this possibility by adding free arginine to disrupt putative intramolecular Arg–Arg pairing interactions. At pH 13.0 (0.1 M KOH), no Arg–Arg pairing is expected since deprotonation removes the aromaticity and disrupts the interaction,<sup>[12]</sup> and TOF values at 1 atm  $\text{H}_2$  were the same with and without added arginine (20 equivalents;  $\text{TOF} \approx 7 \text{ s}^{-1}$ ; Figure S8). However, upon decreasing the pH of these solutions to 0.5, catalysis in the solution containing added arginine proceeded at  $45 \text{ s}^{-1}$  while the control solution having no added arginine had a TOF of  $145 \text{ s}^{-1}$ . Similar results were observed for solutions with added guanidinium-HCl instead of free arginine. These results suggest that intramolecular Arg–Arg interactions may play a role in promoting turnover in  $[\text{Ni}^{\text{II}}(\text{P}^{\text{Cy}_2\text{N}^{\text{Arg}}_2})_2]^{8+}$ . Adding free arginine (up to 100 equivalents) to solutions already at low pH (pH 5.0 in this case) did not influence turnover (Figure S9), suggesting that the Arg–Arg interaction is stable once formed.

Arginine introduces two unique functional groups into the  $[\text{Ni}^{\text{II}}(\text{P}^{\text{Cy}_2\text{N}^{\text{Arg}}_2})_2]^{2+}$  complex: the carboxyl groups and the guanidines. Both of these functional groups could influence the kinetics of the possible rate-controlling chemical steps in the catalytic cycle ( $\text{H}_2$  activation or proton movement; steps 1–3, Figure 4), determined from a combination of experimental and computational studies of similar complexes.<sup>[24]</sup> The first-order dependence on  $\text{H}_2$  pressure observed at all pH values, indicates that in this case rate control resides with the addition (Figure 4, step 1) and/or subsequent heterolytic cleavage (Figure 4, step 2) of  $\text{H}_2$ . Consequently, the arginine functional groups must influence one or both of these processes. With both  $[\text{Ni}^{\text{II}}(\text{P}^{\text{Cy}_2\text{N}^{\text{Arg}}_2})_2]^{8+}$  and the parent  $[\text{Ni}^{\text{II}}(\text{P}^{\text{Cy}_2\text{N}^{\text{Gly}}_2})_2]^{4+}$ , the increase in TOF with decreasing pH has an inflection point at the  $\text{pK}_a$  of the carboxylic acids (Figure 2). A similar inflection point is seen with the  $[\text{Ni}^{\text{II}}(\text{P}^{\text{Cy}_2\text{N}^{\text{Arg}}_2})_2]^{8+}$  complex at the  $\text{pK}_a$  of the guanidine groups. These observations indicate that the rate of  $\text{H}_2$  addition and heterolytic cleavage, and therefore the turnover frequency, is influenced by the protonation states of both the carboxyl and guanidinium groups. We examine contributions from each of these groups in the following paragraphs.

The first step of  $\text{H}_2$  activation is the formation of the dihydrogen adduct (Figure 4), an intermediate not observed but predicted based on previously reported theoretical studies.<sup>[24b,25]</sup> With  $[\text{Ni}^{\text{II}}(\text{P}^{\text{Cy}_2\text{N}^{\text{Gly}}_2})_2]^{4+}$  under conditions where the carboxyl groups were fully deprotonated, the

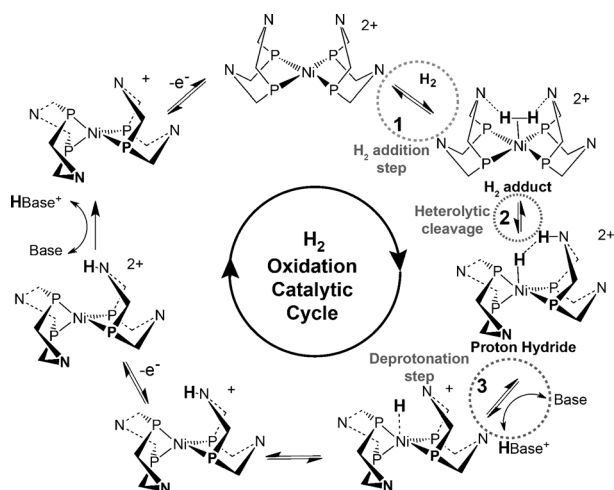


**Figure 4.** The catalytic cycle for  $[\text{Ni}(\text{P}^{\text{R}}_2\text{N}^{\text{R}'}_2)_2]^{2+}$  complexes.<sup>[24b,25]</sup>  $\text{H}_2$  oxidation occurs clockwise. For  $[\text{Ni}^{\text{II}}(\text{P}^{\text{Cy}}_2\text{N}^{\text{Arg}_2})_2]^{8+}$ ,  $\text{COO}^-$  may influence  $\text{H}_2$  addition (1), heterolytic cleavage (2), and/or deprotonation (3) while Arg–Arg interactions may assist  $\text{H}_2$  addition (1) and/or heterolytic cleavage (2) but are unlikely to directly deprotonate (3). The steps are highlighted by gray dotted circles.

voltammetric data under  $\text{N}_2$  showed a shift in the  $\text{Ni}^{\text{III/I}}$  redox couple to more negative potentials. This stabilization of  $\text{Ni}^{\text{II}}$  with respect to  $\text{Ni}^{\text{I}}$  was argued to originate from the intramolecular binding of  $\text{COO}^-$  to  $\text{Ni}^{\text{II}}$ , which under catalytic conditions would compete with the binding of  $\text{H}_2$ , decreasing the TOF at higher pH values.<sup>[7]</sup> Similar voltammetry is observed for  $[\text{Ni}^{\text{II}}(\text{P}^{\text{Cy}}_2\text{N}^{\text{Arg}_2})_2]^{8+}$  (Figure S3B), suggesting that  $\text{COO}^-$  binding may compete with  $\text{H}_2$  addition in this system as well. Another possibility is that the dependence of TOF on pH for both complexes arises from a stable  $\text{COO}^- \cdots \text{H}^+\text{N}$  salt bridge having both electrostatic and hydrogen-bonding components.<sup>[26]</sup> This interaction would hinder amine participation in the addition or heterolytic cleavage of  $\text{H}_2$  (Figure 4, steps 1 and 2). Under acidic conditions, protonation of the carboxyl group would remove the electrostatic component of this interaction, freeing the pendant amine for heterolytic cleavage.

Turnover is faster with  $[\text{Ni}^{\text{II}}(\text{P}^{\text{Cy}}_2\text{N}^{\text{Arg}_2})_2]^{8+}$  than with  $[\text{Ni}^{\text{II}}(\text{P}^{\text{Cy}}_2\text{N}^{\text{Gly}_2})_2]^{4+}$ , indicating that the guanidinium groups in  $[\text{Ni}^{\text{II}}(\text{P}^{\text{Cy}}_2\text{N}^{\text{Arg}_2})_2]^{8+}$  further enhance activity. In enzymes, the guanidinium groups on arginine residues buried within the protein scaffold can participate directly as Brønsted bases due to a reduced  $\text{pK}_a$  induced from the protein environment.<sup>[27]</sup> This is not the case here, since  $\text{pK}_a$  measurements indicate that the guanidines are fully protonated under most of the catalytic conditions tested.

The TOF is higher under conditions favoring intramolecular Arg–Arg interactions. The Arg–Arg interaction could influence  $\text{H}_2$  activation by changing the position of the pendant amines with respect to Ni, stabilizing the addition of  $\text{H}_2$  (Figure 4, step 1)<sup>[24c]</sup> or facilitating its heterolytic cleavage (Figure 4, step 2).<sup>[24b]</sup> Structural and computational studies have shown that the most stable ligand configurations in  $[\text{Ni}^{\text{II}}(\text{P}^{\text{R}}_2\text{N}^{\text{R}'}_2)_2]^{2+}$  complexes place at least one of the pendant amines close to Ni, which is critical for fast turnover.<sup>[8,24b,d]</sup>

Similar metallocyclic diphosphine complexes that do not have sterically enforced amine positioning (e.g.  $[\text{Ni}(\text{PNP})_2]^{2+}$ ) are much less active.<sup>[8,24d]</sup> However, computational studies indicate that even with the positioning introduced by the  $\text{P}_2\text{N}_2$  ring, the equilibrium  $\text{Ni} \cdots \text{N}$  distance is still larger than optimal for the direct transfer of a proton between Ni and N (coupled with electron transfer) during catalysis, and that deflecting the N atom toward Ni by only 0.29 Å could afford up to a 500-fold increase in the rate constant for this concerted process.<sup>[28]</sup> While positioning effects have not been evaluated for the heterolytic cleavage of  $\text{H}_2$ , moderate changes in the  $\text{Ni} \cdots \text{N}$  distance would also be expected to affect the rate of this reaction. Similar sensitivity to proton transfer distance has been proposed for other catalytic systems, including Photosystem II.<sup>[29]</sup> Structural studies are ongoing to more fully evaluate this interaction.

Another interpretation consistent with the high observed turnover frequencies at low pH values is that increased positive charge on the complex, rather than the presence of protons, stabilizes the dihydrogen adduct. Consistent with this interpretation is the positive shift of the overlapping  $\text{Ni}^{\text{III/I}}$  and  $\text{Ni}^{\text{II/I}}$  couples seen in the stoichiometric voltammetry under  $\text{N}_2$  as the pH is decreased (Figure S3B). This positive shift is reflective of a destabilization of the  $\text{Ni}^{\text{II}}$  relative to the  $\text{Ni}^{\text{I}}$  which would favor reduction of Ni by  $\text{H}_2$ . However, this scenario does not explain the dependence of the turnover frequency on the order in which the acid and free arginine are added. If overall charge were the only factor, this dependence would not be expected. Indeed, adding free arginine would have no effect, as is observed for the control complex,  $[\text{Ni}^{\text{II}}(\text{P}^{\text{Cy}}_2\text{N}^{\text{Gly}_2})_2]^{4+}$ . The role of the protonated guanidines is likely complex, and may involve multiple contributions, including localizing water molecules that are proposed to stabilize Arg–Arg interactions.<sup>[12b]</sup> Computational and experimental studies examining the nature of the Arg–Arg interaction are underway, but regardless of the specific mechanism, the presence of guanidinium groups in the outer coordination sphere provides a significant enhancement in catalytic activity.

The overpotentials,<sup>[30]</sup> which quantify the energy wasted per turnover, correlate with the carboxyl protonation state in both  $[\text{Ni}^{\text{II}}(\text{P}^{\text{Cy}}_2\text{N}^{\text{Arg}_2})_2]^{8+}$  and  $[\text{Ni}^{\text{II}}(\text{P}^{\text{Cy}}_2\text{N}^{\text{Gly}_2})_2]^{4+}$ .<sup>[7]</sup> The overpotential for both complexes decreases with pH over the range 14–3 (shown in Figure 2 for  $[\text{Ni}^{\text{II}}(\text{P}^{\text{Cy}}_2\text{N}^{\text{Arg}_2})_2]^{8+}$ ), becomes invariant with pH from 3 to 1, then increases again below pH 1. If both proton and electron transfer steps are fast compared to turnover and reversible, then the ratio of their forward and reverse rates will change with pH and potential as expected for an equilibrium system. The value of  $E_{\text{cat}/2}$  obtained in the potential sweep experiment will then increase by 59.1 mV per unit decrease in pH, as predicted by the Nernst equation. The equilibrium potential for  $\text{H}_2$  oxidation/evolution shows the same pH dependence, and so the overpotential at  $E_{\text{cat}/2}$  will be invariant with pH, as noted with the  $\text{H}_2$ -evolving catalyst  $[\text{Ni}(\text{P}^{\text{Ph}}_2\text{N}^{\text{Bn}_2})_2]^{2+}$  in acetonitrile.<sup>[31]</sup> If either proton or electron transfer is slow compared to turnover, then  $E_{\text{cat}/2}$  will not respond as an equilibrium potential, resulting in higher overpotentials, as observed when the carboxyl groups are deprotonated ( $\text{pH} > 3$ ). This suggests



that the hypothesized salt bridge interferes with proton and/or electron movement as well as H<sub>2</sub> addition. Overpotentials increase both below pH=1 and also with increased H<sub>2</sub> pressure, in both cases tracking substantial increases in TOF, suggesting that turnover becomes fast enough under these conditions that the proton and/or electron transfer steps are no longer under equilibrium control. The collective data illustrate that while the turnover frequency depends on H<sub>2</sub> activation in these systems, energy efficiency can be improved by optimizing the movement of protons and electrons.

Received: February 11, 2014

Published online: May 12, 2014

**Keywords:** amino acid catalysts · bioinspired catalysts · H<sub>2</sub> oxidation · homogeneous electrocatalysis · nickel complex

- [1] J. Y. Yang, S. E. Smith, T. Liu, W. G. Dougherty, W. A. Hoffert, W. S. Kassel, M. R. DuBois, D. L. DuBois, R. M. Bullock, *J. Am. Chem. Soc.* **2013**, *135*, 9700–9712.
- [2] a) S. W. Ragsdale, *Chem. Rev.* **2006**, *106*, 3317–3337; b) T. E. Creighton, *Proteins: Structures and Molecular Properties*, 2nd ed., Freeman, New York, **1993**.
- [3] W. J. Shaw, *Catal. Rev. Sci. Eng.* **2012**, *54*, 489–550.
- [4] J. C. Fontecilla-Camps, A. Volbeda, C. Cavazza, Y. Nicolet, *Chem. Rev.* **2007**, *107*, 4273–4303.
- [5] Overpotential is the excess potential required to drive a redox reaction at a desired rate, beyond the equilibrium potential for that reaction.
- [6] a) A. K. Jones, E. Sillery, S. P. Albracht, F. A. Armstrong, *Chem. Commun.* **2002**, 866–867; b) C. Madden, M. D. Vaughn, I. Diez-Perez, K. A. Brown, P. W. King, D. Gust, A. L. Moore, T. A. Moore, *J. Am. Chem. Soc.* **2012**, *134*, 1577–1582.
- [7] A. Dutta, S. Lense, J. Hou, M. Engelhard, J. A. S. Roberts, W. J. Shaw, *J. Am. Chem. Soc.* **2013**, *135*, 18490–18496.
- [8] A. D. Wilson, R. H. Newell, M. J. McNevin, J. T. Muckerman, M. R. DuBois, D. L. DuBois, *J. Am. Chem. Soc.* **2006**, *128*, 358–366; W. J. Shaw, M. L. Helm, D. L. DuBois, *Biochim. Biophys. Acta Bioenergetics* **2013**, *1827*, 1123–1139.
- [9] The charge of [Ni<sup>II</sup>(P<sup>Cy</sup><sub>2</sub>N<sup>Arg</sup><sub>2</sub>)]<sup>8+</sup> changes as a function of pH from 2– (pH=14) to 8+ (pH=0). For simplicity, we will call it consistently [Ni<sup>II</sup>(P<sup>Cy</sup><sub>2</sub>N<sup>Arg</sup><sub>2</sub>)]<sup>8+</sup>.
- [10] S. Cukierman, *Biochim. Biophys. Acta Bioenerg.* **2006**, *1757*, 876–885.
- [11] a) A. Chaumont, M. Baer, G. Mathias, D. Marx, *ChemPhys-Chem* **2008**, *9*, 2751–2758; b) I. Efimov, S. K. Badyal, C. L. Metcalfe, I. Macdonald, A. Gumiero, E. L. Raven, P. C. E. Moody, *J. Am. Chem. Soc.* **2011**, *133*, 15376–15383.
- [12] a) J. Vondrášek, P. E. Mason, J. Heyda, K. D. Collins, P. Jungwirth, *J. Phys. Chem. B* **2009**, *113*, 9041–9045; b) Z. Y. Zhang, Z. J. Xu, Z. Yang, Y. T. Liu, J. A. Wang, Q. Shao, S. J. Li, Y. X. Lu, W. L. Zhu, *J. Phys. Chem. B* **2013**, *117*, 4827–4835.
- [13] a) The observation of a plateau at large potentials is consistent with electron transfer that is rapid relative to turnover; b) J. M. Savéant, *Elements of Molecular and Biomolecular Electrochemistry: An Electrochemical Approach to Electron Transfer Chemistry*, Wiley, Hoboken, **2006**.
- [14] V. Artero, M. Fontecave, *Chem. Soc. Rev.* **2013**, *42*, 2338–2356.
- [15] a) J. Saveant, E. Vianello, *Electrochim. Acta* **1965**, *10*, 905–920; b) R. Nicholson, I. Shain, *Anal. Chem.* **1964**, *36*, 706–723.
- [16] Protonation of one of the two amines on each ligand acidifies the other, so a maximum of two of the four pendant amines may be protonated at pH=7.
- [17] M. O'Hagan, M. H. Ho, J. Y. Yang, A. M. Appel, M. Rawkowski DuBois, S. Raugei, W. J. Shaw, D. L. DuBois, R. M. Bullock, *J. Am. Chem. Soc.* **2012**, *134*, 19409–19424.
- [18] a) A. L. De Lacey, V. M. Fernandez, *Chem. Rev.* **2007**, *107*, 4304–4330; b) J. A. Cracknell, K. A. Vincent, F. A. Armstrong, *Chem. Rev.* **2008**, *108*, 2439–2461.
- [19] With the oxidizing acid HClO<sub>4</sub>, activity decreased by 37% after 24 h.
- [20] A. D. Wilson, K. Frazee, B. Twamley, S. M. Miller, D. L. DuBois, M. Rakowski DuBois, *J. Am. Chem. Soc.* **2008**, *130*, 1061–1068.
- [21] K. Frazee, A. D. Wilson, A. M. Appel, M. Rakowski DuBois, D. L. DuBois, *Organometallics* **2007**, *26*, 3918–3924.
- [22] M. L. Reback, B. Ginovska-Pangovska, M.-H. Ho, A. Jain, T. C. Squier, S. Raugei, J. A. S. Roberts, W. J. Shaw, *Chem. Eur. J.* **2013**, *19*, 1928–1941.
- [23] B. Gao, T. Wyttenbach, M. T. Bowers, *J. Phys. Chem. B* **2009**, *113*, 9995–10000.
- [24] a) A. D. Wilson, R. K. Shoemaker, A. Miedaner, J. T. Muckerman, D. L. DuBois, M. R. DuBois, *Proc. Natl. Acad. Sci. USA* **2007**, *104*, 6951–6956; b) S. Raugei, S. Chen, M.-H. Ho, B. Ginovska-Pangovska, R. J. Rousseau, M. Dupuis, D. L. DuBois, R. M. Bullock, *Chem. Eur. J.* **2012**, *18*, 6493–6506; c) M. Dupuis, S. Chen, S. Raugei, D. L. DuBois, R. M. Bullock, *J. Phys. Chem. A* **2011**, *115*, 4861–4865; d) M. Rakowski DuBois, D. L. DuBois, *Chem. Soc. Rev.* **2009**, *38*, 62–72.
- [25] M. Rakowski DuBois, D. L. DuBois, *C. R. Chim.* **2008**, *11*, 805–817.
- [26] T. Wyttenbach, M. Witt, M. T. Bowers, *Int. J. Mass Spectrom.* **1999**, *182–183*, 243–252.
- [27] Y. V. Guillén Schlippe, L. Hedstrom, *Arch. Biochem. Biophys.* **2005**, *433*, 266–278.
- [28] a) L. E. Fernandez, S. Horvath, S. Hammes-Schiffer, *J. Phys. Chem. Lett.* **2013**, *4*, 542–546; b) S. Horvath, L. E. Fernandez, A. V. Soudackov, S. Hammes-Schiffer, *Proc. Natl. Acad. Sci. USA* **2012**, *109*, 15663–15668.
- [29] a) L. Hammarström, S. Styring, *Energy Environ. Sci.* **2011**, *4*, 2379–2388; b) M.-T. Zhang, T. Irebo, O. Johansson, L. Hammarström, *J. Am. Chem. Soc.* **2011**, *133*, 13224–13227.
- [30] Quantified as the difference between  $E_{cat/2}$  and the condition-dependent equilibrium potential for the reaction being mediated, see the Supporting Information.
- [31] A. M. Appel, D. H. Pool, M. O'Hagan, W. J. Shaw, J. Y. Yang, M. Rakowski DuBois, D. L. DuBois, R. M. Bullock, *ACS Catal.* **2011**, *1*, 777–785.